

Prostasome Self-Fusion Studied by Atomic Force Microscopy

Marco Girasole,^{*,†} Antonio Cricenti,[†] Carlotta Rindone,[†] Agostina Congiu-Castellano,[‡] Giuseppe Arienti,[§] Carla Saccardi,^{||} and Carlo A. Palmerini^{||}

CNR—Istituto di Struttura della Materia, Via Fosso del Cavaliere 100, 00133 Rome, Italy, Dipartimento di Fisica, Università “La Sapienza” ed Unità INFN di Roma 1, p. le A. Moro 7, 00185 Rome, Italy, Dipartimento di Medicina Interna e Scienze Endocrine e Metaboliche, Sezione di Biochimica, Via del Giochetto, 06122 Perugia, Italy, and Dipartimento di Scienze Biochimiche e Biotecnologie Molecolari, Università di Perugia, Via del Giochetto, 06122 Perugia, Italy

Received: November 6, 2002; In Final Form: March 10, 2003

We used atomic force/lateral force microscopy (AFM/LFM) and the transfer of a lipophilic fluorescent dye (octadecylrhodamine G, R₁₈) to study the morphology and fusion of human prostasomes at pH values ranging between 5 and 8. The AFM data revealed that the mean diameter of untreated prostasomal vesicles was about 200 nm, but a second prostasome population with a diameter of about 400 nm is also present. This second population increased upon exposing the vesicles to low pH values. The AFM/LFM characterization revealed the smoothness of the prostasome surface and showed that the larger vesicles were fused prostasomes, as also indicated by the relief of R₁₈ self-quenching.

Introduction

Prostasomes are membrane vesicles secreted by the human prostate gland.¹ Their lipid composition is peculiar; cholesterol is present in high amounts as is sphingomyelin, whereas phosphatidylcholine is less abundant.² Many proteins of their surface possess catalytic activity or are involved in the immune response.^{3,4} Among the physiological roles of prostasomes we cite the enhancement of sperm motility,⁵ the liquefaction of semen,⁶ and immunosuppression.^{7,8} Prostasomes fuse to spermatozoa, whose membrane lipid composition is largely different, through a pH-dependent and protein-dependent mechanism.⁹ Recent results seem to support the idea that prostasomes may undergo self-fusion.¹⁰

Atomic force microscopy (AFM) is a scanning probe technique that provides three-dimensional imaging at nanometer scale resolution of surface structures, independently on their conducting/insulating characteristics, thus allowing a noninvasive and quantitative analysis of sample morphology. Furthermore, coupling AFM with lateral force microscopy (LFM) allows one to detect modulation of the friction between tip and sample and, therefore, to reveal chemical inhomogeneity as well as to map the surface distribution of different material. Measurements can be performed in water environment or in air and do not require the covering of the surface with metals, a feature that makes this technique an ideal tool for studying biological samples.^{11,12}

In the present paper we studied prostasomes exposed to different pH values and measured the relief of R₁₈ fluorescence self-quenching to establish whether prostasomes may aggregate or fuse among themselves. This is the first morphometric study of prostasomes, and the statistical analysis on the size and shape and distinguishing between aggregation and fusion processes

reported in the present paper are a few straightforward applications of AFM and LFM peculiarities.

Material and Methods

Prostasomes were obtained from fresh human semen, as previously described,⁹ and subsequently separated from amorphous material by gel filtration on a Sephadex G-200 column (1.5 × 30 cm). Prostasomes were not retained by the column and were collected with the void volume, V₀. They were finally harvested by centrifugation at 105000g × 120 min and suspended in 30 mM Tris + 130 mM NaCl, adjusted to pH 7.4 with HCl (3–4 mg of protein mL⁻¹). The sample was characterized as previously described.^{13–16}

For AFM observation, prostasomes were mixed with 0.32 M sucrose + 20 mM MES or 2 mM HEPES at the required pH and incubated at room temperature for 10 min. Prostasomes were then harvested by centrifugation at 105000g × 60 min. The pellet was fixed with 2% paraformaldehyde for 10 min at room temperature. The biological material was then collected by centrifugation at 10000g × 20 min, washed twice in PBS buffer, and then twice again with distilled water. Prostasomes were eventually suspended in distilled water to have 300 μg protein mL⁻¹. Aliquots (50 μL) of this suspension were layered on the glass slide.

Although the final target of AFM studies is to analyze the sample under physiological conditions, fixing or staining procedure are still often used in AFM and sometimes are unavoidable. For instance, some kind of fixing is used when statistical analysis of an evolving system is required (see ref 17) or, like in our case, when dealing with a sample that may hardly be attached to a substrate in solution environment. In these cases fixing is important if one wants to avoid undesired chemical modification of either sample (that would impair the LFM approach) or substrate (that could, in principle, affect the protein-dependent self-fusion of prostasomes). Indeed, most of the papers devoted to study of liposomes or prostasomes by microscopy have been carried out on air-dried samples.

* Corresponding author. E-mail: marco.girasole@ism.cnr.it.

[†] CNR—Istituto di Struttura della Materia.

[‡] Università “La Sapienza” ed Unità INFN di Roma 1.

[§] Sezione di Biochimica.

^{||} Università di Perugia.

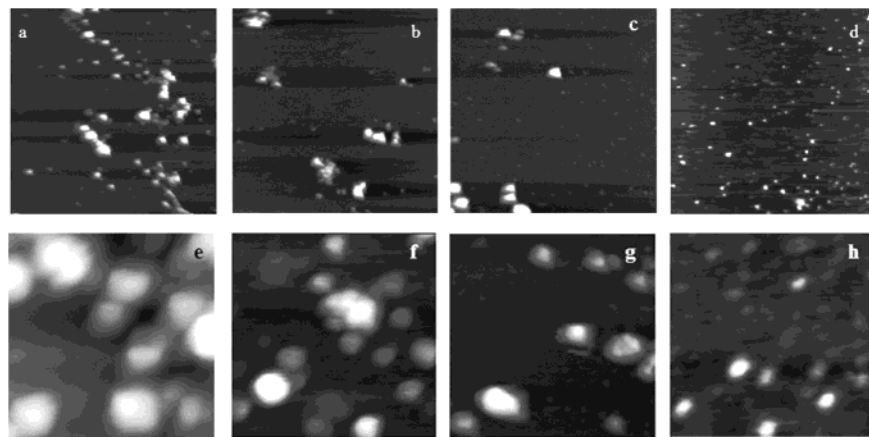


Figure 1. AFM images of prostasomes at different pH values, respectively: pH 5 (panel a = $8\ \mu\text{m} \times 8\ \mu\text{m}$ and panel e = $2\ \mu\text{m} \times 2\ \mu\text{m}$), pH 6 (panel b = $10\ \mu\text{m} \times 10\ \mu\text{m}$ and panel f = $2\ \mu\text{m} \times 2\ \mu\text{m}$), pH 7 (panel c = $10\ \mu\text{m} \times 10\ \mu\text{m}$ and panel g = $2\ \mu\text{m} \times 2\ \mu\text{m}$), pH 8 (panel d = $8\ \mu\text{m} \times 8\ \mu\text{m}$ and panel h = $2\ \mu\text{m} \times 2\ \mu\text{m}$). Images at two different magnification (not the same areas) are reported in order to show the different appearance of the samples.

Moreover, despite the debates concerning the use of air-drying techniques for cell fixing, the sample preparation method used in the present paper has been accepted for AFM studies (and similar methods are used in other microscopy techniques including photoelectron spectromicroscopy and routine cell fixing in hospital labs), for it has been proved able to fix the morphology without inducing morphological artifacts.^{18–25} Such a point has been, in particular, carefully controlled by comparing the morphological characteristics of liposomes, Raji cells, and RBC prepared with the present method and with several different protocols^{26,27} (including the protocol for scanning electron microscopy) obtaining negligible differences or general agreement.

The insertion of R₁₈ (Molecular Probes, Eugene, OR) into prostasomes was performed as described before by utilizing a probe-to-lipid ratio of 1:200 or less.^{9,28} Prostasomal suspensions ($100\ \mu\text{L}$, 0.2–0.3 mg of protein of labeled prostasomes and similar amounts of unlabeled vesicles) were mixed with 0.32 M sucrose + 20 mM MES or 2 mM HEPES, at the required pH. The fluorescence signal (λ_{ex} , 560 nm; λ_{em} , 580 nm) was examined with a Perkin-Elmer LS 50B spectrophotofluorimeter to assess the relief of octadecyl-Rhodamine fluorescence self-quenching, which monitors the lipid mixing.⁹ The extent of fusion (taking as 100% the complete intermixing of lipid phases) was calculated as previously discussed.²⁹

The AFM instrument was described in detail elsewhere.³⁰ The AFM images were collected in air at room temperature (relative humidity 35%). The microscope worked in the weak repulsive regime of contact mode, with a force smaller than 1 nN from zero cantilever deflection. We used gold-coated cantilevers (Park Scientific Instruments) with a spring constant of 0.032 N/m and carrying an integrated Si₃N₄ tip. Topographic and lateral force images were acquired simultaneously with a typical scan rate of about 5–6 s/row. An analysis of the noise in the images was performed. As a consequence of the results, we considered 1.2 nm, corresponding to three times the rms of the (Gaussian) noise, as the minimum feature unambiguously attributable to a physical structure.

Results and Discussion

We studied the prostasome–prostasome fusion process and characterized, for the first time, the surface of single, aggregated, and fused prostasomes. Aggregation and fusion are elicited by exposing prostasomes at slightly acidic pH values (5.0, 6.0, 7.0,

and 8.0, as reference). The analysis were performed by AFM/LFM and by following the relief of R₁₈ fluorescence self-quenching.

Figure 1 shows AFM images, at two different magnifications, taken after the exposure of prostasomes to different pH values: pH 5 (panels a, e), 6 (b, f), 7 (c, g) and 8 (d, h). Two populations of prostasomes can be observed at any pH value: a smaller one with a diameter of about 120–200 nm and a larger one with a diameter of 350–600 nm. The size and the distribution of the vesicles depends on the pH as, at pH 8, prostasomes mostly appear like a random distribution of small sized particles, whereas at pH 5 and 6, we observe larger vesicles, mainly in the form of clusters. An intermediate situation is present at pH 7. Larger sized aggregated particles with diameters on the microns scale occur, although not often, at the higher pH.

Concerning to the pH-dependent fusion mechanism, the data obtained with both AFM and transfer of lipophilic fluorescent dye are in good agreement (see Figure 2a,b). Fluorescence measurements (Figure 2a) show a pH-dependent transfer of the R₁₈ from a vesicle population to the other, and this has been interpreted as prostasome fusing among themselves. Correspondingly (Figure 2b), an analysis of the two prostasome populations cited above shows their occurrence with different percentages, depending on the pH values. At pH 8 there is a high percentage of prostasomes with a diameter of 120–200 nm, whereas, as consequence of the fusion, at pH 5 the population with 350–600 nm predominate

Further analysis demonstrates the occurrence of three different prostasome sub-populations: single, aggregated, and fused. Figure 3 shows the topography, cross section, and LF image of the three subpopulations and illustrates the capability of AFM images to partition the observed elements among these population. A single prostasome (Figure 3a) has a diameter of about 200 nm measured at its half-height. In the aggregate form (Figure 3b), single prostasomes are still visible; in fact, cross sections show that the sum of R of every single unit is about the distance between the centers. The fused vesicles (Figure 3c) mostly appear as bigger vesicles (diameter 450 nm).

The usefulness of the lateral force images^{17,31} is evident in Figure 3, which reveals the absence of nonhomogeneous regions on the prostasome surfaces and allows one to unambiguously identify the single units constituting fused and aggregated complexes. Moreover, analysis of LF images also reveals that the surface of prostasome is smooth, a characteristic also

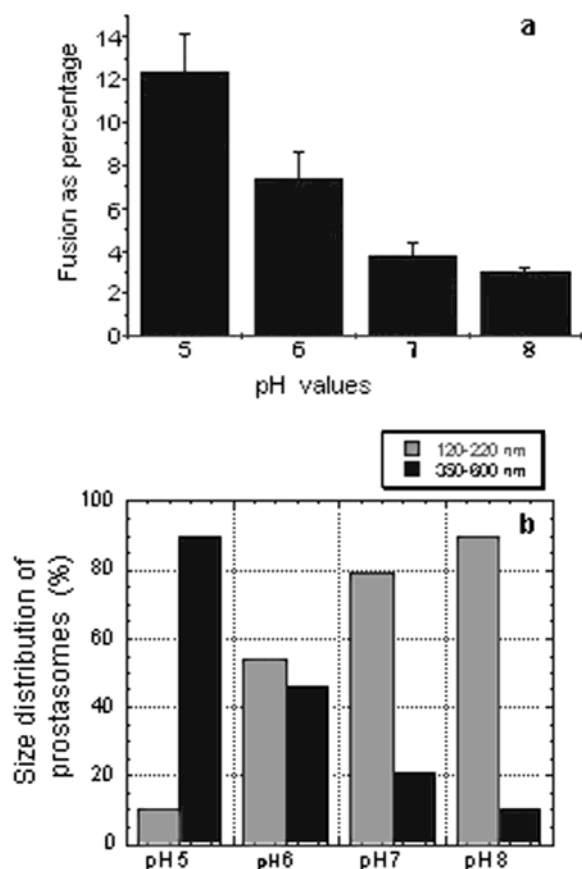


Figure 2. Panel a: dependence of fusion (as seen through the R_{18} method) on pH values. Panel b: percentages of prostasome's population at different pH values by the analysis of AFM images. Statistics has been built by analyzing, at each pH, 10 images of $8/10\ \mu\text{m}$. Each image carries 60–250 prostasomal units.

confirmed by quantitative topographic images, and that it was maintained at any tested pH value (i.e. was a common characteristic to either single and fused prostasomes). To show the smoothness of the prostasomes surface, Figure 4 shows three-dimensional AFM images of a single (panel a) and a fused (panel b) prostasome. The corresponding cross sections are reported as well.

Furthermore, LF images provide a clear distinction between aggregated and fused prostasomes, by showing clustered prostasomes and prostasomes showing larger diameter. Although the extent of aggregation or of fusion vary from sample to sample, as a consequence of the used pH values and of the variability of biological material, the diameter of fused prostasomes is always about 450 nm, which corresponds to the fusion of two or three single units (only rarely four). Lateral force images allow one to distinguish between fused and aggregated prostasomes, a distinction that was not possible to make with other methods exploited until now. Since we observed clusters of two or (prevalently) three aggregated vesicles and much larger (450 nm or more) vesicles, we can propose a phenomenological mechanism for the self-fusion process: prostasomes may, in a first step, aggregate in groups of two or three and then fuse. The formation of vesicles of about 450 nm seems to form a quite stable state, since fused particles resulting from the fusion of four or (particularly) five prostasomes were detected in lesser extent in our experimental conditions. Therefore, the initial processes of aggregation and of fusion would preferably imply the intervention of two or three prostasomal vesicles. The much larger (on the microns scale)

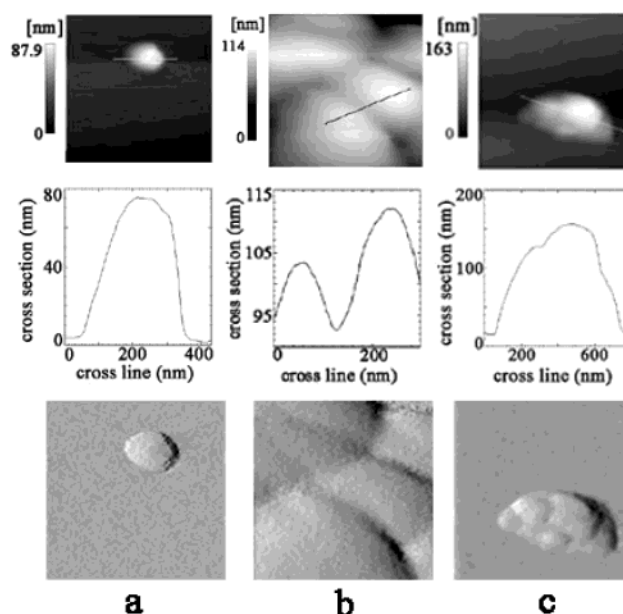


Figure 3. AFM images of single, aggregated, and fused prostasomes. Panel 3a, from top to bottom: topography (960 nm × 960 nm), cross section, and lateral force images of a single prostasome; the diameter measured at its half-height is 220 nm, the LF image reveals the absence of nonhomogeneous regions. Panel 3b, from top to bottom, topography (500 nm × 500 nm), cross section, and lateral force images of an aggregate; by cross section we can see that the sum of R of every unit is about the distance between the centers. Panel 3c, from top to bottom, topography (1.2 μm × 1.2 μm), cross section, and lateral force images of fused prostasomes. The diameter is 450 nm and by LF image we can still identify the single fused units. The surfaces of the single or fused prostasomes did not show any relevant changes due to fusion.

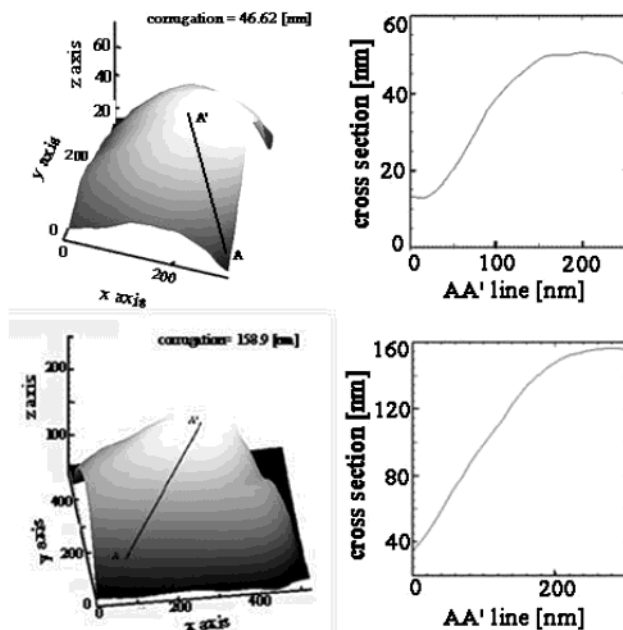


Figure 4. 3D-AFM images and related cross sections. The surfaces of the single (a) or fused prostasomes (b) was always quite smooth and, in particular, did not show any relevant change due to fusion. It is worth noting how three-dimensional quantitative analysis can be very suitable to detect morphological details and to distinguish between different aggregation/fusion states of prostasomes.

fused vesicles detected (although not often) in our samples could then result from the subsequent fusion of the 450 nm particles.

It is worth noting that the above presented interpretation has to be considered, at the present state, just as a speculative

hypothesis, and an effect due to the adhesion of prostasomes on the surface that could affect the fusion process cannot be excluded to occur.

Distinguishing between aggregated and fused vesicles may explain the differences noted between Figure 2b, reporting about 90% of fused prostasomes at pH 5, and Figure 2a, which shows the fusion percentage has a maximum at pH 5 of about 13%. In Figure 2b, in fact, no distinction is made between aggregated and fused prostasomes, where the transfer of the dye implies a mixing of the lipid phases of vesicles.

In addition, the formula used in this paper to calculate the percentage of fusion²⁹ is

$$F_u = F_l (1 + r/u)$$

where F_u is the percentage of fusion, F_l is the fluorescence dequenching, and r and u are the percentage of loaded and unloaded membranes, respectively, as lipid phosphorus. This implies the collision of two particles and may underestimate the extent of fusion if the collision occurs among more than two vesicles, as shown by AFM.

It is remarkable that the present AFM and R_{18} (in solution) data are basically in agreement with the previous light scattering (in solution) and SEM data¹⁰ about the average size of particles and the occurrence of fusion process. Since, however, these techniques are complementary to each other, is not surprising that our quantitative measurements show an even larger difference between the mean size of fused and unfused vesicles that, in turns, allows one to refine the previous results. Furthermore, the general agreement between the results obtained by using different techniques provide itself a validation of the different protocols of sample preparation and seems to suggest that sample–substrate adhesion effects do not play a major role in the fusion process.

The present study, interesting per se, could also be considered as the necessary background knowledge for studying the prostasomes–spermatozoa fusion mechanism under physiological conditions.

Acknowledgment. This work has been partially supported by grants from Italian MURST (Ministero dell'Università e della Ricerca Scientifica e Tecnologica) contract no. 9902018391.

References and Notes

- (1) Ronquist, G.; Brody, I. *Biochim. Biophys. Acta* **1985**, *822*, 203–218.
- (2) Arvidson, G.; Ronquist, G.; Wikandere, G.; Ojteg, A. C. *Biochim. Biophys. Acta* **1989**, *984*, 167–173.
- (3) Fabiani, R. *Upsala J. Med. Sci.* **1994**, *99*, 73–111.
- (4) Fabiani, R.; Johansson, L.; Lundkvist, O.; Ulmsten, U.; Ronquist, G. *Eur. J. Obstet. Gynecol. Reprod. Biol.* **1994**, *57*, 181–188.
- (5) Stegmayr, B.; Berggren, P. O.; Ronquist, G.; Hellman, B. *Scand. J. Urol. Nephrol.* **1982**, *16*, 199–203.
- (6) Lilja, H.; Laurell, C. B. *Scand. J. Clin. Lab. Invest.* **1984**, *44*, 447–452.
- (7) Kelly, R. W.; Holland, P.; Skibinski, G.; Harrison, C.; McMillan, L.; Hargreave, T.; James, K. *Clin. Exp. Immunol.* **1991**, *86*, 550–556.
- (8) Skibinski, G.; Kelly, R. W.; Harkiss, D.; James, K. *Am. J. Reprod. Immunol.* **1992**, *28*, 97–103.
- (9) Arienti, G.; Carlini, E.; Palmerini, C. A. *J. Membr. Biol.* **1997**, *155*, 89–94.
- (10) Bordin, F.; Cametti, C.; De Luca, F.; Carlini, E.; Palmerini, C. A.; Arienti, G. *Arch. Biochem. Biophys.* **2001**, *396*, 10–15.
- (11) Bustamante, C.; Vesenka, J.; Tang, C. L.; Rees, W.; Guthold, M.; Keller, R. *Biochemistry* **1992**, *31*, 22–28.
- (12) Shao, Z.; Mou, J.; Czajkowski, D. M.; Yang, J.; Yuan, J. Y. *Adv. Phys.* **1996**, *45*, 1–86.
- (13) Arienti, G.; Polci, A.; Carlini, E.; Palmerini, C. A. *FEBS Lett.* **1997**, *410*, 343–346.
- (14) Arienti, G.; Carlini, E.; Polci, A.; Cosmi, E. V.; Palmerini, C. A. *Arch. Biochem. Biophys.* **1998**, *358*, 391–395.
- (15) Lowry, O. H.; Rosebrough, N. J.; Farr, A. L.; Randall, R. J. *J. Biol. Chem.* **1951**, *193*, 265–272.
- (16) Bartlett, G. R. *J. Biol. Chem.* **1959**, *234*, 466.
- (17) Girasole, M.; Cricenti, A.; Generosi, R.; Silvestri, I.; Gazzaniga, P.; Pozzi, D.; Agliano, A. M. *Appl. Phys. Lett.* **2001**, *78*, 1143–1145.
- (18) Nakanishi, M.; Noguchi, A. *Adv. Drug Deliv. Rev.* **2001**, *52*, 197–207.
- (19) Kawaura, C.; Noguchi, A.; Furuno, T.; Nakanishi, M. *FEBS Lett.* **1998**, *421*, 69–72.
- (20) Truneh, A.; Machy, P.; Horan, P. K. *J. Immunol. Methods* **1987**, *100*, 59–71.
- (21) Paclet, M. H.; Coleman, A. W.; Vergnaud, S.; Morel, F. *Biochemistry* **2000**, *39*, 9302–9310.
- (22) Garcia, C. R. S.; Takeuchi, M.; Yoshioka, K.; Miyamoto, H. *Imaging Plasmodium falciparum-infected ghost and parasite by AFM. J. Struct. Biol.* **1997**, *119*, 92–98.
- (23) Zhang, P. C.; Bai, C.; Huang, Y. M.; Zhao, H.; Fang, Y.; Wang, N. X.; Li, Q. *Scanning Microsc.* **1995**, *9(4)*, 981–988.
- (24) De Stasio, G.; Casalbore, P.; Pallini, R.; Gilbert, B.; Sanita, F.; Ciotti, M. T.; Rosi, G.; Festinesi, A.; Larocca, L. M.; Rinelli, A.; Perret, D.; Mogk, D. W.; Perfetti, P.; Mehta, M. P.; Mercanti, D. *Cancer Res.* **2001**, *61*, 4272–4277.
- (25) Sciola, L.; Cogoli-Greuter, M.; Cogoli, A.; Spano, A.; Pippia, P. *Adv. Space Res.* **1999**, *24(6)*, 801–805.
- (26) Girasole, M.; Cricenti, A.; Generosi, R.; Congiu-Castellano, A.; Pozzi, D.; Pasquali, E.; Lisi, A.; Santoro, N.; Grimaldi, S. *Appl. Phys. A* **1998**, *67*, 219–223.
- (27) Girasole, M.; Cricenti, A.; Generosi, R.; Congiu-Castellano, A.; Boumis, G.; Amiconi, G. *J. Microscopy* **2001**, *204*, 46–52.
- (28) Hoekstra, D.; de Boer, T.; Klappe, K.; Wilschut, J. *Biochemistry* **1984**, *23*, 5675–5681.
- (29) Corazzi, L.; Pistolesi, R.; Arienti, G. *J. Neurochem.* **1991**, *56*, 207–212.
- (30) Cricenti, A.; Generosi, R. *Rev. Sci. Instrum.* **1995**, *66*, 2843–2847.
- (31) Ruan, J. A.; Bhushan, B. *J. Appl. Phys.* **1994**, *76*, 5022–5035.